

MALAYSIAN JOURNAL OF ANALYTICAL SCIENCES

ANALIS

Journal homepage: https://mjas.analis.com.my/

Research Article

Preparation and characterization of WO₃/g-C₃N₄ composite for photodegradation of 4-hydroxybenzoquinone under low UV-light intensity

Nik Fatin Nabihah Atiqah Nik Ramli¹, Hamizah Mokhtar^{1*}, Zul Adlan Mohd Hir^{2,3*}, and Hartini Ahmad Rafaie⁴

¹Civil Engineering Studies, College of Engineering, Universiti Teknologi MARA Pahang Branch, 26400 Bandar Tun Abdul Razak Jengka, Pahang, Malaysia

²Faculty of Applied Sciences, Universiti Teknologi MARA Cawangan Pahang Branch, 26400 Bandar Tun Abdul Razak Jengka, Pahang, Malaysia

³Catalysis for Sustainable Water and Energy Nexus Research Group, School of Chemical Engineering, College of Engineering, Universiti Teknologi MARA, 40450 Shah Alam, Selangor, Malaysia

⁴Centre of Foundation Studies, Universiti Teknologi MARA, Selangor Branch, Dengkil Campus, 43800 Dengkil, Selangor, Malaysia

*Corresponding author: hamizah1161@uitm.edu.my, zuladlan@uitm.edu.my

Received: 14 September 2023; Revised: 30 August 2024; Accepted: 18 November 2024; Published: 1 February 2025

Abstract

Organic ultraviolet (UV) filter is considered as an emerging contaminant through their detection in many aquatic environments. The presence of organic UV filters tends to give high risks towards the human endocrine and environmental ecological systems under long exposure. The existing wastewater treatment approaches such as coagulation, filtration, and adsorption are unable to remove completely this type of contaminant from the water bodies due to the difficulties in breaking down the chemical structures. However, heterogeneous photocatalytic system has been chosen as the most promising approach to combat such contaminants which relies on the presence of reactive radical species and can be operated at room temperature and pressure. The current work focused on the preparation and characterization of WO₃/g-C₃N₄ composite photocatalysts and evaluation of its photocatalytic activity towards 4-Hydroxybenzoquinone (4-HBQ) under low intensity UV-C irradiation (9 W). The composite photocatalyst was prepared via facile mixing approach, by varying the mass ratio of g-C₃N₄ ranging from 0.1 g to 0.5 g. The photocatalyst was successfully characterized by using Fourier Transform Infrared (FTIR) and X-Ray diffraction (XRD) analyses. The highest degradation percentage of 79.58% is obtained through WG3 composite photocatalyst with pseudo-first-order rate constant-C₃N₄ of 0.0077 min⁻¹. Furthermore, WG3 shows the best performance, which is stabled for a course of 180 min. This study showed that the composite photocatalyst has the high potential for application in larger wastewater treatment processes.

Keywords: g-C₃N₄; 4-Hydroxybenzoquinone; Photocatalyst; Water Treatment; WO₃

Introduction

Exogeneous endocrine disrupting chemicals (EDCs) from numerous sectors have the potential to pollute water which has become a major ecotoxicological concern. The life of aquatic organisms and people has been significantly challenged by the widespread presence of such compounds in water bodies, even in extremely low concentrations (ngL-1) [1]. Due to EDCs' distinctive chemical and physical properties and their capacity to disrupt hormonal systems, their process of elimination is particularly difficult and complicated. The discharge of untreated pollutants into downstream water supplies as a result of

conventional wastewater treatment systems' inability to effectively remove EDCs contaminants from urban wastewater poses a serious threat to both persons and the environment. Adsorption, sophisticated oxidation methods, and bioremediation are just a few of the quick and significant advancements in wastewater treatment that have been achieved to address the issue of water contamination involving EDCs and have shown to increase their removal. However, these methods are unattractive, and because of a number of restrictions like high energy demand and high running costs, their applicability have been severely restricted [2]. According to this perspective, semiconductor-

mediated photocatalysis has been suggested as a useful method to deal with these poisonous organic contaminants in the wastewaters.

Additionally, they include prospective qualities like cheap cost, energy conversion, photochemical stability, and non-toxicity [3]. When a substance comes into contact with photons with a high enough energy level, free radical processes begin to operate, activating the chemical reaction known photocatalysis. A photocatalyst is a substance that absorbs light and serves as a catalyst for chemical reactions. In essence, all photocatalysts are semiconductors. A semiconducting substance will produce an electron-hole pair when exposed to light in a process known as photocatalysis. The usage of efficient light-harvesting, environmentally friendly and non-toxic semiconductor materials are necessary for the real application of water treatment as to provide safe access to potable water and to safeguard human health [4]. Semiconductors function as photocatalysts because they can conduct electricity even at ambient temperature in the presence of light. An electron (e⁻) in the valence band of a photocatalyst absorbs photon energy when it is exposed to light of the desired wavelength (with adequate energy) and is stimulated to the conduction band. In this procedure, the valence band develops a positive hole (h⁺). This mechanism creates the photo excitation state and produces the electron-hole pairs. This excited electron is employed to reduce an acceptor, in which a hole is employed to oxidise molecules of the donor. The significance of photocatalysis resides in the fact that a photocatalyst simultaneously creates series of oxidation and reduction environment.

Recently, tungsten trioxide (WO₃), an n-type semiconductor, has been chosen as the promising photocatalyst to degrade several organic pollutants in water [5]. The advantages of this semiconductor include great absorption in the UV/visible spectrum, resilience in acidic and oxidative environments, low cost, low toxicity, good chemical stability, and superior optical performance. Due to its low photocatalytic activity for reduction events and quick charge carrier recombination, WO3 has a conduction band potential. Their electrical characteristics support a larger range of applications, such as the treatment of water [6]. Despite its ability to respond to UV/visible light, pure WO₃ has two fundamental drawbacks which are high rate of charge carrier recombination and low CB edge location. Since CB of WO₃ is +0.5 eV, no photocatalytic application is able to effectively perform the reduction process [7]. According to this perspective, it is essential to build photocatalysts that can be fully utilized under UV/visible light. The photocatalytic performance of WO₃ can be enhanced by changing its surface and electrical characteristics through doping with various substances.

Since it offers a promising means of avoiding deteriorating Fermi Level Alignment, restricting electron-hole recombination, narrowing the band gap and shifting the absorbance to the visible region ($\lambda \ge$ 400 nm), heterojunctions of WO₃ with other materials are currently receiving other additionally particular attention [8]. The efficiency of semiconductors in diverse applications is greatly influenced by the stability of Fermi level migration at the interface during heterojunction manufacturing. To validate the direction of the charge migration in various photocatalytic processes, it is necessary to carefully investigate the stability of Fermi level migration [9]. It is important to note that several carbon nanomaterials are particularly desirable as a dopant or addition to WO₃ for improving photocatalytic and photo-electrocatalytic performance due to their good conductivity and strong adsorption capacity. A hydrated WO3 crystal was doped with carbon and placed in an interstitial location. In addition, the electrical and optical characteristics of WO₃ have been altered by non-metals such N, S, I, and P to enhance photocatalytic performance. These dopants produce positive effects that are comparable to those of carbon nanostructures.

Among metal-free materials, g-C₃N₄ appears to be the most flexible due to its earth-abundant, low band gap of 2.7 eV, inexpensive and acts as a fascinating conjugated material capability in the development of nanomaterials that can improve the physicochemical properties of WO₃. In addition, g-C₃N₄ is well known for its high adsorption capacitance and visible-lightinduced activity, which are important for creating an efficient and long-lasting remediation system for removing organics from aqueous media [10]. WO₃ can benefit from having g-C₃N₄ as a dopant because this system was initially employed to boost WO₃ performance when it was paired with g-C₃N₄ [11]. One of the most important approaches for band gap engineering that can improve photocatalytic characteristics is the coupling of low band gap materials, such as WO₃ with g-C₃N₄ to create heterostructures. The issue with the transfer path of photo-excited charge carriers in the photocatalytic system still exists in the majority of common heterojunctions, whereby any electrons or holes left on the semiconductors could readily recombine. As a result, the problem may be resolved, and the redox potential is increased by the heterojunction mechanism in which is projected to result in an opposing flow of electrons from the WO₃ conduction band to g-C₃N₄. In contrast towards the performance of the isolated oxides, the photogenerated electrons and holes can be spatially distributed in two distinct crystalline phases of g-C₃N₄ grafted with WO₃ and charge recombination is thereby prevented. This results in timely and efficient photocatalytic activity towards organic pollutants.

In this work, WO₃/g-C₃N₄ composite photocatalysts were prepared by a simple mixing approach with the use of commercially available WO3 nanoparticles. A series of composites with different ratios were prepared by simply adjusting the mass of as-prepared g-C₃N₄. The photocatalytic performances of the composites were tested towards Hydroxybenzoquinone (4-HBQ) in aqueous solution under low-intensity UV light irradiation (9W). The functional groups and structural of the WO₃/g-C₃N₄ composite photocatalysts were investigated by employing Fourier transform infrared (FTIR) and Xray diffraction (XRD), respectively. The resulted heterojunction photocatalytic material is expected to have a significantly photocatalytic enhancement for water treatment process.

Materials and Methods Materials

Commercial tungsten trioxide (WO_3 , 99%), melamine ($C_{18}H_{10}N_2O_4$, 99%), and 4-Hydroxybenzoquinone (4-HBQ, $C_6H_4O_3$, 98%) were supplied by Sigma-Aldrich (Selangor, Malaysia). All chemicals were utilized as received, without refinement and deionized water was used throughout the experiments.

Preparation of g-C₃N₄

Melamine, $C_{18}H_{10}N_2O_4$ (2.5g) was grinded for about 30 min at room temperature. Next, the sample was subjected to condensation process at 500° C in a muffle furnace for about 2 h with the heating rate of 5° C/min in a close crucible. The resultant yellow powder of g- C_3N_4 was obtained and stored for later use.

Preparation of WO₃/g-C₃N₄ composite photocatalyst

 WO_3/g - C_3N_4 composite photocatalyst was prepared by mixing the two materials through different mass ratios of g- C_3N_4 . First, 0.1~g of WO_3 was mixed with 0.1~g of previously prepared g- C_3N_4 and dispersed in a deionized water (50 mL) with continuous stirring for 1~h. The collected light-yellow sample was dried in the oven at $80^{\circ}C$ overnight and labelled as WG1. The

same procedure was repeated with different masses of $g\text{-}C_3N_4$. The composition of the prepared photocatalysts is presented in **Table 1.**

Characterizations

The functional groups of the prepared samples were analyzed through Fourier Transform Infrared (FTIR) within the range of 450 cm⁻¹ to 4000cm⁻¹ on the Perkin Elmer infrared spectrometer by using Attenuated Total Reflection (ATR) Pellet technique. X-ray powder diffractometer (XRD, PANalytical X'PERT-Pro MPD) was employed to identify the sample's crystallinity degree and phases with Cu K α 1 radiation (λ = 1.540 Å, 45 kV, and 40 mA) in the 2θ range of 10–70° with a scanning speed of 2°/min.

Evaluation of photocatalytic performances

The calibration plot of the target pollutant (4-Hydroxybenzoquinone, 4-HBQ) with concentration ranging from 5 to 25 mg/L in an aqueous solution was carried out. The linear equation was determined from the calibration plot by measuring absorbance of each sample at a maximum wavelength ($\lambda_{max} = 283$ nm). Typically, time dependence of the concentration loss of a degraded compound is used to assess the photocatalytic effectiveness in this system. A 250 mL glass photoreactor was used to conduct the photocatalytic activity of 4-HBQ in an aqueous solution with the aid of a low intensity of UV-C light (9 W, $\lambda = 254$ nm). The photoreactor was filled with 100 mL of the working solution with a known concentration and 0.2 g of photocatalyst. Prior to beginning the photodegradation testing, photoreactor will be left in the dark for 30 min to achieve adsorption-desorption equilibrium. Air will then be continuously supplied to the photoreactor at a flow rate of 4 L/min to guarantee the presence of dissolved oxygen in the solution. The photoreactor will then be irradiated with UV-C light. After that, the liquid sample (5-10 mL) was collected at regular intervals of 30 min and filtered to get rid of the photocatalyst. A Perkin Elmer UV-vis spectroscopy was used to monitor the impact of changing the mass ratios of WO₃/g-C₃N₄ on the photodegradation of 4-HBQ. The following equations were used in this investigation to compute the degradation percentage.

Table 1. Compositions for the preparation of WO₃/g-C₃N₄ composite photocatalysts

WO ₃ (g)	g-C ₃ N ₄ (g)	Photocatalyst
0.1	0.1	WG1
0.1	0.2	WG2
0.1	0.3	WG3
0.1	0.4	WG4
0.1	0.5	WG5

Degradation percentage (%) =
$$\frac{(c_0 - c_t)}{c_0} \times 100\%$$
 (Eq. 1)

Where C_0 is the concentration of 4-HBQ before irradiation and C_t is the concentration of 4-HBQ at time 't'

Results and Discussion

Fourier transform infrared spectroscopy (FTIR) analysis

FTIR techniques were used for characterization in order to better inquire about the functional groups and chemical bond states of the composite photocatalysts (**Figure 1**). The stretching modes of W-O-W and O-W-O in tungsten oxide have been correlated to an absorption band with a broad in the wavelength range of 500 cm⁻¹ to 950 cm⁻¹ for the pure WO₃ sample, as illustrated in Figure 1(a) [14]. The narrow spectral band at 812 cm⁻¹ for the pure g-C₃N₄ sample results

from the s-triazine units' breathing mode as shown in Figure 1(b). The peaks in the range of 1200 to 1600 cm⁻¹ (1397.54, 1313.64, and 1225.21 cm⁻¹) are connected to usual vibrational broadening of CN heterocycles [15]. The extensive absorption spectrum at 3100 to 3600 cm⁻¹ could be attributed by the material's residual water and the O-H vibratory stretching of uncondensed -NH2. The composite material's absorption peak values are comparable to the values of pure g-C₃N₄ which proves its chemical composition is unaltered by the addition of pure WO₃ [16]. However, the intensity of the WO₃/g-C₃N₄ composite is much broader than the pure g-C₃N₄ at about 800 cm⁻¹ and 3100 cm⁻¹ to 3600 cm⁻¹ as illustrated in Figure 1 (c). This is due to the absorption peaks overlapping with each other. The intensity of the broader absorption spectrum in the region of 500 to 950 cm⁻¹ has been reduced by considering WO₃ content added is relatively low.

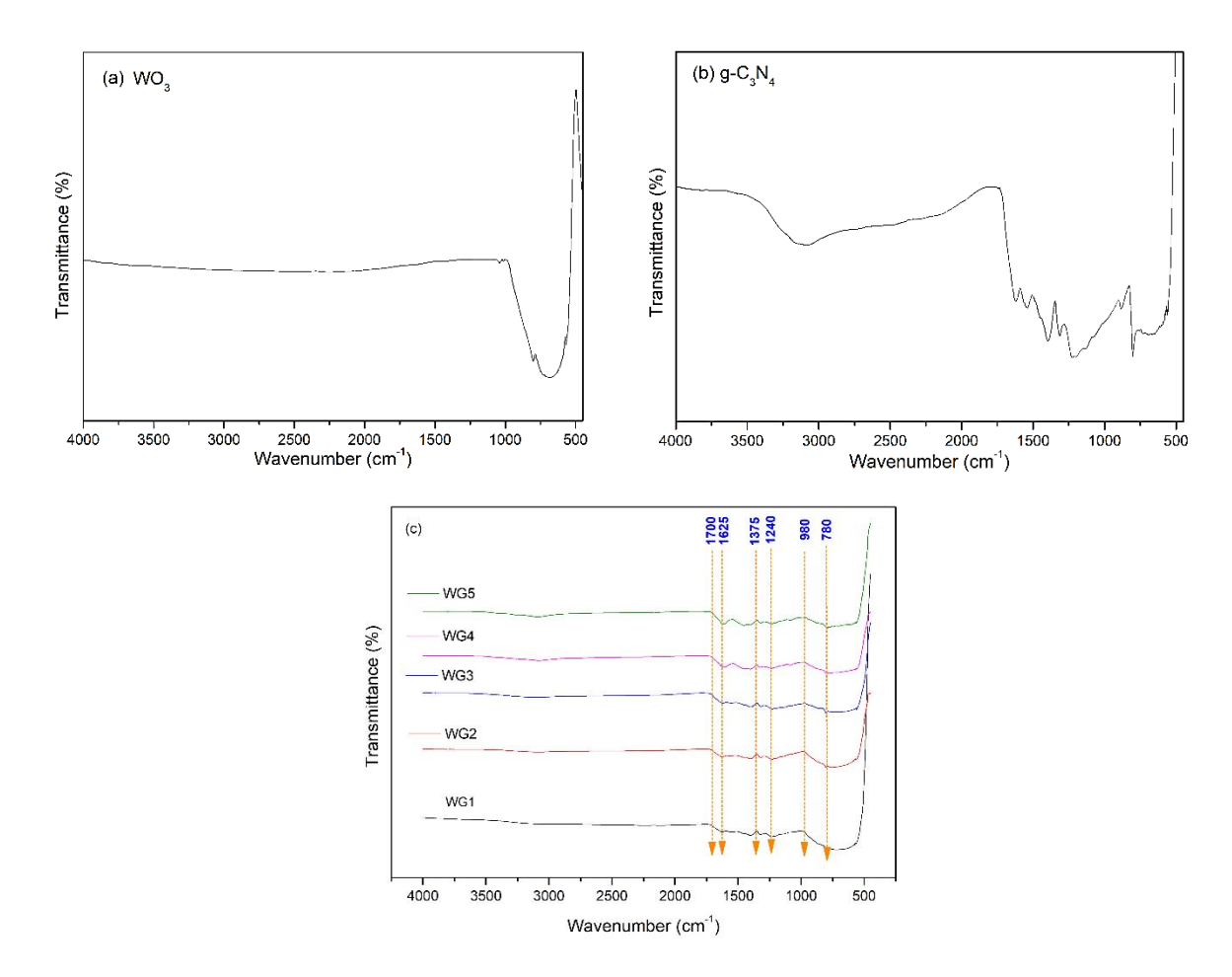


Figure 1. FTIR spectra of (a) WO₃, (b) $g-C_3N_4$, and (c) WO₃/ $g-C_3N_4$ composite photocatalysts with different mass ratios

X-ray diffraction (XRD) analysis

The crystallinity and phase compositions of the pure WO_3 , pure $g-C_3N_4$, and $WO_3/g-C_3N_4$ composite photocatalysts with different mass ratios were investigated, as shown in Figure 2. It can be seen that the peaks of WO₃ (ICDD No. 20-0483) are displayed at 22.55° (001), 24.03° (110), 28.59° (101), 33.42° (111), 34.28° (200), 41.62° (201), 45.21° (211), 46.76° (002), 49.27° (220), 50.11° (102), 53.25° (112) and 54.94° (221) in Figure 1(a). These peaks' sharpness indicates that WO₃ nanostructures have a high degree of crystallinity. This characteristic is categorized as a tetragonal crystal system [17]. Meanwhile, the (100) and (002) planes of g-C₃N₄ are identified at 13.83° and 23.70°. The peak at 13.83° denotes the in-plane structural repeating unit of Nbridged tri-s-triazine and the peak at 23.70° is corresponding to the assembled of the aromatic systems between layers as displayed in Figure 2(b) [18]. It is clear from the pattern that the g-C₃N₄ structure is not considerably altered during the heat treatment with no presence of impurity peaks that may be attributable to the phase of the melamine cyanurate or other derivative stages of carbon nitride [19]. According to ICDD No. 36-1694, this attribute is classified as an orthorhombic crystal system.

A comparable pattern to that of WO₃ is displayed after integrating g-C₃N₄ with WO₃, demonstrating strong interaction between the two materials. The spectra does not clearly show the peaks of g-C₃N₄ since the peak of g-C₃N₄ is shifted from 23.70° to 28.04° which indicates g-C₃N₄ is partially covered by WO₃ [20]. The g-C₃N₄/WO₃ composites' phase analysis shows, synthetization of heterojunction photocatalyst causes such a variety phases of tungsten oxide to occur. The composites with the highest tungsten oxide content (ICDD No. 42-0452) comprise of WO₃ with a hexagonal crystalline structure. When g-C₃N₄ content was added up to 0.5 g (WG5), monoclinic -WO3 is the predominant tungsten-containing phase and wellhydrated tungsten oxide WO3 becomes crystallized when g-C₃N₄ content increases as shown in Figure 2 (c). Overall, the crystallinity and phase compositions of the tungsten oxide are slightly affected by the addition of g-C₃N₄ in the composite photocatalysts' structures [19].

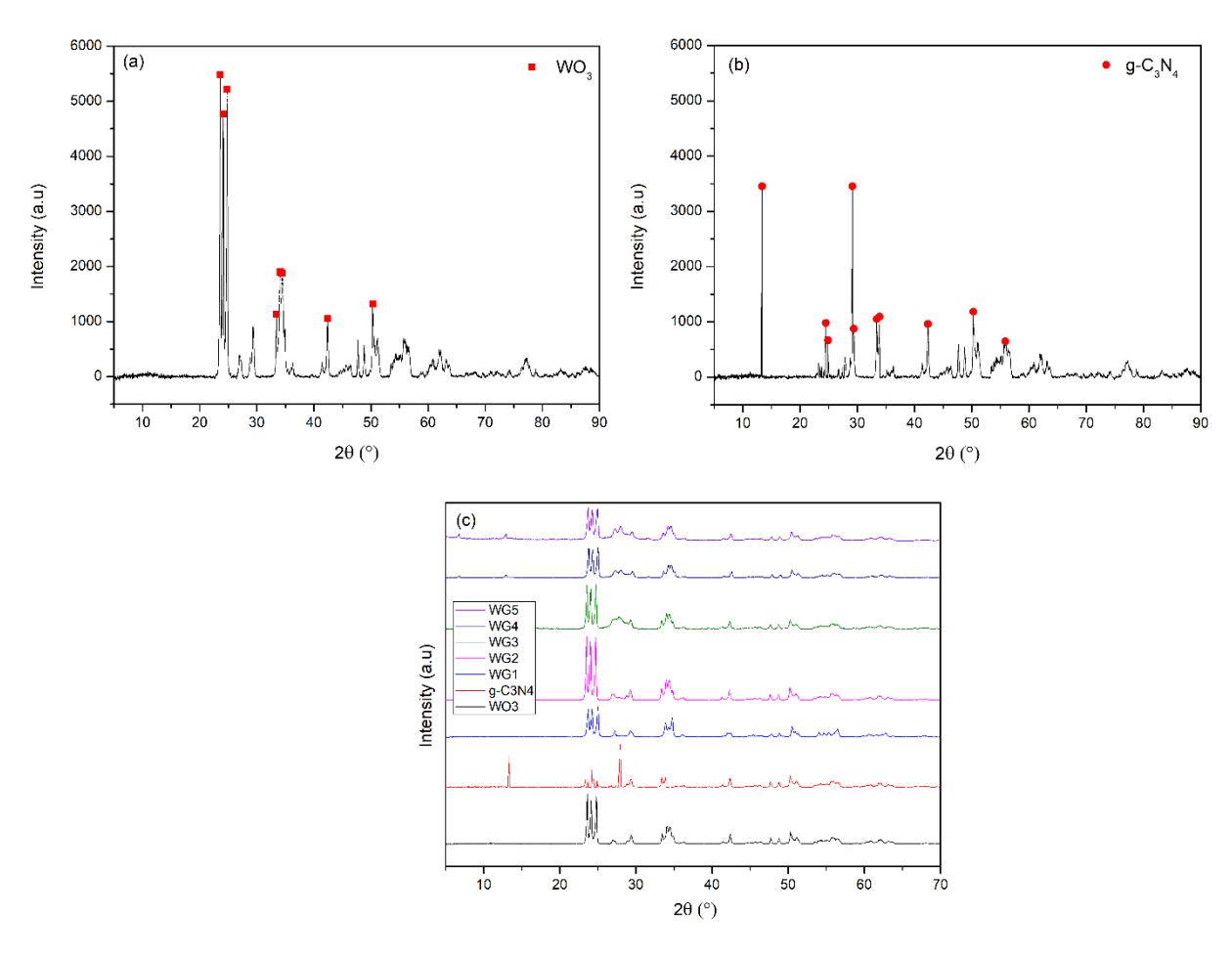


Figure 2. XRD pattern of (a) WO₃, (b) g-C₃N₄, and (c) WO₃/g-C₃N₄ composite photocatalysts with different mass ratios

Evaluation of photocatalytic performances

Based on their ability to degrade the Hydroxybenzophenone (4-HBQ) when exposed to UV light, the photocatalytic performances for all prepared photocatalysts were assessed. degradation percentage of 4-HBQ is plotted as a function of time, over the course of 180 min (Figure 3). From the results, pure WO_3 and $g-C_3N_4$ show such a high degradation percentage which are 68.09% and 58.38%, respectively. This proves that pure WO₃ and g-C₃N₄ are exhibiting semiconductor properties which can be used under the exposure of UV light. However, when combining both materials at 1:1 (WG1) and 1:2 (WG2) ratios, the degradation percentage records much lower values. Interestingly, the composite photocatalyst exhibits the highest degradation percentage of 79.58% at ratio 1:3 (WG3). Nonetheless, increasing the mass of g-C₃N₄ up to 0.5 g deteriorating the photocatalytic performances down to 26.34% and 11.04% for 1:4 and 1:5 ratios, respectively. Theoretically, the photocatalysts are enthused to produce photoinduced electron (e-) and positive holes (h+) in the conduction band (CB) and valence bands (VB) when exposed to light irradiation (photons) with energy equal to or much higher than their specific band gap [4]. Next, adsorbed oxygen and water react with those charge carriers in a sequence of redox reactions to further form reactive radicals species known as superoxide radical anions (•O₂-) and hydroxyl radicals (•OH), respectively [21]. These reactive radical species will then be able to target 4-HBQ molecules that are on the photocatalyst surface. As a result, it will mineralize the contaminants into benign species like water and carbon dioxide molecules. The best photocatalyst of WG3 might produce decent heterojunction between WO3 and g-C₃N₄ with appropriate mass ratio. The heterojunction

formation may trap the photoinduced electrons, thus reducing the electron-hole recombination and simultaneously enhancing the photocatalytic activity [22]. Moreover, the greater photocatalytic activity of the WG3 photocatalyst can potentially be attributed to the increase in charge separation caused by expanding the photoexcitation's energy range. Their distinctive physicochemical features after underwent considerable modification could also contribute into such enhancement. On the other hand, WG1, WG2, WG4, and WG5 have lower degradation percentages which are due to the rapid recombination process between photoinduced electron and hole pairs on the catalyst's surfaces. This is in good agreement with previously reported study which also used WO₃/g-C₃N₄ binary photocatalyst [23]. Therefore, the synergistic interaction between WO₃ and g-C₃N₄ are looked into by considering their appropriate mass ratio which is essential to construct a potential composite photocatalyst with outstanding heteroiunction formation.

Kinetic studies

The Langmuir-Hinshelwood model was employed, which can be demonstrated by the pseudo-first-order model at low concentrations as it is the most frequently used model in order to assess the kinetics of photocatalytic systems [24][25][26]. In order to fit the photocatalytic data, a pseudo-first-order kinetic equation, as shown in Eq. (2) was used [27]:

$$\ln\left(\frac{c_o}{c_t}\right) = k_{obs}t$$
(Eq. 2)

Where k_{obs} indicates the pseudo-first order rate constant and t as irradiation time.

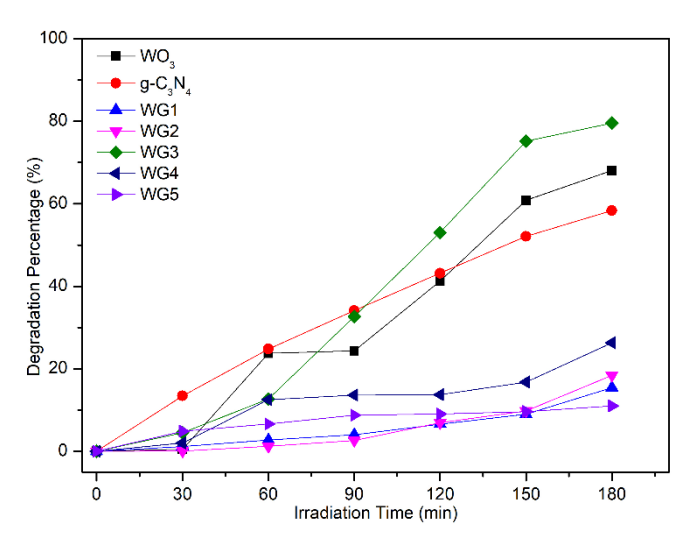


Figure 3. Degradation percentage of 4-HBQ in aqueous solution by using pure WO₃, pure g-C₃N₄, and WO₃/g-C₃N₄ composite photocatalysts with different mass ratios

Pseudo-first-order kinetics regulate the photocatalytic disintegration of the pollutant which is 4-HBQ and the corresponding linear graph is shown in Figure 4. The rate constants of each photocatalysts are determined using the linear plots. The data correspond with the pseudo-first-order kinetic model, showing a linear connection with $\ln \left(\frac{c_o}{c_t}\right)$ versus t, with R^2 are nearest to 1 [28]. The outcomes are consistent with a study that found first-order kinetics establish the photocatalytic degradation of 4-HBQ with pure WO₃, $g-C_3N_4$ and $WO_3/g-C_3N_4$ photocatalysts (Figure 4 and Table 2). Numerous research on the degradation of organic pollutants have been reported by using first-order and pseudo-firstorder kinetic models [29].

Comparison on the removal efficiency of UV filters

UV filters have traditionally been removed from water by using a variety of techniques. Some research looks into photocatalysis which breaks down UV filter by using light to activate a photocatalyst. A comparison of several photocatalytic methods for UV filter degradation is shown in Table 1. These include more recent applications like graphitic carbon nitride (g-C₃N₄) and other composite materials as well as more well-known semiconductors such as zinc oxide (ZnO) and titanium dioxide (TiO2). The sources of light also differ in which ranging from UV lamps that are focused to artificial sunlight. The amount of irradiation time applied can vary and affect the length of the treatment. The wide range of degradation efficiencies emphasizes the significance photocatalytic process optimization.

One particular method that shows a lot of potential is the degradation 4-hydroxybenzoquinone by using a composite photocatalyst consisting of WO_3 and g- C_3N_4 . This study used a remarkably low-power (9W) light source as activation and the sol-gel method of catalyst synthesisation. Even with a moderate 180-minute irradiation period, the degradation efficiency is noteworthy 79.58%. This indicates that WO_3/g - C_3N_4 has a great deal of potential for practical application because it performs better in milder environments than other methods.

Large scale water treatment facilities can save the operating costs by using low-power light sources. Apart from that, WO_3/g - C_3N_4 makes use of low UV light, which is more plentiful, and possibly cost-free resource compared to higher watt UV lamp or mercury lamp. Although it is not the best, it successfully removes a significant amount of UV filter and still has opportunity for improvement.

Table 3 below offers some insights into the wide range of photocatalytic UV filter degradation scenarios. It is crucial to keep in mind that practical applications take other aspects into an account. These include the cost, stability and recyclability of catalyst. Due to its effectiveness in milder conditions, $WO_3/g-C_3N_4$ approach shows a great promise for addressing UV filter removal overall as it consists strong candidate for additional research and possible industrial implementation.

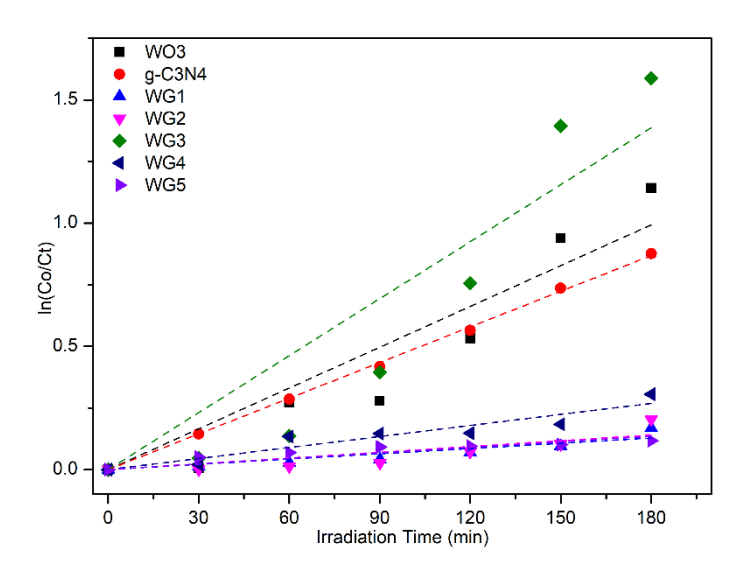


Figure 4. Kinetic data for degradation of 4-HBQ in aqueous solution by using pure WO₃, pure $g-C_3N_4$, and WO₃/ $g-C_3N_4$ composite photocatalysts with different mass ratios

Table 2. Degradation percentage and kinetics data of all photocatalysts

Photocatalyst	Degradation Percentage (%)	Kobs (min-1)	Correlation Factor, R ²	
Pure WO ₃	68.09	0.0055	0.9431	
Pure g-C ₃ N ₄	58.38	0.0048	0.9995	
WG1	15.45	0.0007	0.9245	
WG2	18.41	0.0008	0.8591	
WG3	79.58	0.0077	0.9319	
WG4	26.34	0.0015	0.9649	
WG5	11.04	0.0008	0.9510	

Table 3. A comparison of the removal; UV filters by using photocatalysts based on previous studies

UV Filters	Photocatalyst	Synthesis Method	Light Source	Irradiation Time (min)	Degradation Efficiency (%)	Reference
Benzophenone-4	TiO ₂ NWs	Hydrothermal	Lightbulbs	180	80%	[12]
2-Phenylbenzmidazole- 5-sulfonic acid	TiO ₂	Co- precipitation	125W mercury UV lamp	1440	100%	[13]
2-Phenylbenzmidazole- 5-sulfonic acid	ZnO	Hydrothermal	125W UV lamp	180	85%	[13]
4- Hydroxybenzoquinone	WO_3/g - C_3N_4	Sol-gel method	9W UV lamp	180	~80	This Study

Conclusion

In this research, a straightforward chemical mixing procedure was used to successfully prepare WO₃/g-C₃N₄ composite photocatalysts which were then examined by using a variety of characterization techniques. High photocatalytic degradation of 4-HBQ under original condition occurred as a result of the synergistic interaction between WO₃ and g-C₃N₄ with appropriate mass ratio of 1:3 (WG3). The degradation percentage obtained was 79.58% with the highest degradation rate of 0.0077 min⁻¹. The appropriate construction of $WO_3/g-C_3N_4$ heterojunction could enhance the photocatalytic responses towards low intensity of UV-C irradiation over the course of 180 min. This photocatalytic material has high potential to be applied for current water remediation process for the elimination of dangerous organic contaminants like 4-HBQ in aqueous solution.

Acknowledgements

This research was funded by Ministry of Higher Education, Malaysia under the Fundamental Research Grant Scheme (FRGS) (Project Number: FRGS/1/2022/TK08/UITM/02/17), and Universiti Teknologi MARA, Malaysia under the UiTM Grant (600-RMC/GPM LPHD 5/3 (166/2021). The authors as well thankfully appreciate the services and facilities

provided by Universiti Teknologi MARA (UiTM) Pahang Branch and UiTM Shah Alam to carry out the laboratory work.

References

- Hir, Z. A. M., and Abdullah, A. H. (2022). Hybrid polymer-based photocatalytic materials for the removal of selected endocrine disrupting chemicals (EDCs) from aqueous media: A review. *Journal of Molecular Liquids*, 361: 119632.
- Brillas, E., and Manuel Peralta-Hernández, J. (2023). Removal of paracetamol (acetaminophen) by photocatalysis and photoelectrocatalysis. A critical review. Separation and Purification Technology, 309: 122982-123026.
- 3. Mano, G., Harinee, S., Sridhar, S., Ashok, M., and Viswanathan, A. (2020). Microwave assisted synthesis of ZnO-PbS heterojuction for degradation of organic pollutants under visible light. *Scientific Reports*, 10(1): 1-14.
- 4. Mukhair, H., Halim Abdullah, A., Adlan Mohd Hir, Z., Syazwani Osman, N., Zainal, Z., and Hong Ngee, L. (2023). In-depth investigation on the photostability and charge separation mechanism of Ag₃PO₄/g-C₃N₄ photocatalyst towards very low visible light intensity. *Journal*

- of Molecular Liquids, 376: 121494.
- Kubacka, A., Caudillo-Flores, U., Barba-Nieto, I., and Fernández-García, M. (2021). Towards full-spectrum photocatalysis: Successful approaches and materials. *Applied Catalysis A*, *General*, 610: 117966-117998.
- 6. Ghanbari Shohany, B., and Khorsand Zak, A. (2020). Doped ZnO nanostructures with selected elements Structural, morphology and optical properties: A review. *Ceramics International*, 46(5): 5507–5520.
- Camposeco, R., Castillo, S., Rodriguez-González, V., Hinojosa-Reyes, M., Medina-Álvares, M. I., and Mejía-Centeno, I. (2018). Promotional effect of Rh nanoparticles on WO₃/TiO₂ titanate nanotube photocatalysts for boosted hydrogen production. *Journal of Photochemistry and Photobiology A: Chemistry*, 353: 114-121.
- 8. Low, J., Yu, J., Jaroniec, M., Wageh, S., and Al-Ghamdi, A. A. (2017). Heterojunction Photocatalysts. *Advanced Materials*, 29(20): 1601694.
- Shandilya, P., Sambyal, S., Sharma, R., Mandyal, P., and Fang, B. (2022). Properties, optimized morphologies, and advanced strategies for photocatalytic applications of WO₃ based photocatalysts. *Journal of Hazardous Materials*, 428: 128218-12843.
- Peleyeju, M. G., and Viljoen, E. L. (2021). WO3-based catalysts for photocatalytic and photoelectrocatalytic removal of organic pollutants from water A review. *Journal of Water Process Engineering*, 40: 101930-101945.
- 11. Alaghmandfard, A., and Ghandi, K. (2022). A comprehensive review of graphitic carbon nitride (g-C₃N₄)-metal oxide-based nanocomposites: potential for photocatalysis and sensing. *Nanomaterials*, 12(294): 1-80.
- Soto-Vázquez, L., Rolón-Delgado, F., Rivera, K., Cotto, M. C., Ducongé, J., Morant, C., Pinilla, S., and Márquez-Linares, F. M. (2019). Catalytic use of TiO₂ nanowires in the photodegradation of Benzophenone-4 as an active ingredient in sunscreens. *Journal of Environmental Management*, 247: 822-828.
- Ahmed, M. B., Johir, M. A. H., Zhou, J. L., Ngo, H. H., Guo, W., and Sornalingam, K. (2017). Photolytic and photocatalytic degradation of organic UV filters in contaminated water. *Green* and Sustainable Chemistry, 6: 85-92.
- Wang, X., Zhu, Z., Jiang, J., Li, R., and Xiong, J. (2023). Preparation of heterojunction C₃N₄/WO₃ photocatalyst for degradation of microplastics in water. *Chemosphere*, 337: 139206-139213.
- 15. Sun, P., Liu, Y., Mo, F., Wu, M., Xiao, Y., Xiao,

- X., Wang, W., and Dong, X. (2023). Efficient photocatalytic degradation of high-concentration moxifloxacin over dodecyl benzene sulfonate modified graphitic carbon nitride: Enhanced photogenerated charge separation and pollutant enrichment. *Journal of Cleaner Production*, 393: 136320-136330.
- Priya, A., Senthil, R. A., Selvi, A., Arunachalam, P., Kumar, C. K. S., Madhavan, J., Boddula, R., Pothu, R., and Al-mayouf, A. M. (2020). A study of photocatalytic and photoelectrochemical activity of as-synthesized WO₃/g-C₃N₄ composite photocatalysts for AO7 degradation. *Materials Science for Energy Technologies*, 3: 43-50.
- 17. Zhang, X., Xinyue, W., Meng, J., Liu, Y., Ren, M., Guo, Y., and Yang, Y. (2021). Robust Z-scheme g-C₃N₄/WO₃ heterojunction photocatalysts with morphology control of WO₃ for efficient degradation of phenolic pollutants. *Separation and Purification Technology*, 255: 117693-117709.
- 18. Jin, Z., Murakami, N., Tsubota, T., and Ohno, T. (2020). Complete oxidation of acetaldehyde over a composite photocatalyst of graphitic carbon nitride and tungsten (VI) oxide under visible-light irradiation. *Applied Catalysis B: Environmental*, 150-151: 479-485.
- Medvedeva, E. D., Kozlov, D. A., Revenko, A. O., and Garshev, A. V. (2023). Synthesis of g-C₃N₄/WO₃ composites under hydrothermal conditions and study of their photocatalytic properties. *Material Proceedings*, 14(17): 1-5.
- Cui, L., Liu, Y., Fang, X., Yin, C., Li, S., Sun, D., and Kang, S. (2018). Scalable and clean exfoliation of graphitic carbon nitride in NaClO solution: Enriched surface active sites for enhanced photocatalytic H₂ evolution. *Green Chemistry*, 20: 37043.
- 21. Abdullah, R. R., Shabeed, K. M., Alzubaydi, A. B., and Alsalhy, Q. F. (2022). Novel photocatalytic polyether sulphone ultrafiltration (UF) membrane reinforced with oxygendeficient tungsten oxide (WO_{2.89}) for Congo red dye removal. *Chemical Engineering Research and Design*, 177: 526-540.
- 22. Shinde, D. R., Tambade, P. S., Chaskar, M. G., and Gadave, K. M. (2017). Photocatalytic degradation of dyes in water by analytical reagent grades ZnO, TiO₂ and SnO₂: A comparative study. *Drinking Water Engineering and Science*, 10: 109-117.
- 23. Ruan, S., Huang, W., Zhao, M., Song, H., & Gao, Z. (2020). A Z-scheme mechanism of the novel ZnO/CuO n-n heterojunction for photocatalytic degradation of Acid Orange 7. *Materials Science in Semiconductor Processing*, 107: 104835-104845.

- 24. Hossaini, H., Moussavi, G., and Farrokhi, M. (2017). Oxidation of diazinon in *cns*-ZnO/LED photocatalytic process: Catalyst preparation, photocatalytic examination, and toxicity bioassay of oxidation by-products. *Separation and Purification Technology*, 174: 320-330.
- Orooji, Y., Tanhaei, B., Ayati, A., Hamidi, S., and Alizadeh, M. (2021). Heterogeneous UV-switchable Au nanoparticles decorated tungstophosphoric acid/TiO₂ for efficient photocatalytic degradation process. *Chemosphere*, 281: 130795-130802.
- Gong, C., Chen, F., Yang, Q., Luo, K., Yao, F., Wang, S., Wang, X., Wu, J., Li, X., Wang, D., and Zeng, G. (2017). Heterogeneous activation of peroxymonosulfate by Fe-Co layered doubled hydroxide for efficient catalytic degradation of Rhoadmine B. Chemical Engineering Journal,

- 321: 222-232.
- 27. Simonin, J. (2016). On the comparison of pseudo-first order and pseudo-second order rate laws in the modeling of adsorption kinetics. *Chemical Engineering Journal*, 300: 254-263.
- 28. Pirsaheb, M., Hossaini, H., Asadi, A., and Jafari, Z. (2022). Enhanced degradation of diazinon with a WO₃-Fe₃O₄/g-C₃N₄-persulfate system under visible light: Pathway, intermediates toxicity and mechanism. *Process Safety and Environmental Protection*, 162: 1107-1123.
- 29. Gmurek, M. (2019). Comparison of radical-driven technologies applied for paraben mixture degradation: mechanism, biodegradability, toxicity and cost assessment. *Environmental Science and Pollution Research*, 26: 37174-37192.